

## Analysis of weak-anchoring effect in nematic liquid crystals

Wei Zhao, Chen-Xu Wu, and Mitsumasa Iwamoto

Department of Physical Electronics, Tokyo Institute of Technology, 2-12-1 O-okayama, Meguro-ku, Tokyo 152-8552, Japan

(Received 3 May 2000)

A generalized Rapini-Papoular-type anchoring energy formula [J. Phys. (Paris) Colloq. **30**, C4-54 (1969)] with two coupling constants is established through a second-order spherical-harmonic expansion. Using this formula, we analyze the threshold and saturation properties of twisted nematic devices with unidirectional planar anchorage, assuming that the azimuthal and polar anchoring strengths are both finite and distinct from each other. We also discuss the voltage-controlled-twist effect [G. P. Bryan-Brown *et al.*, Nature (London) **392**, 365 (1998)]. It is shown that the predicted behavior is consistent with the experimental observations.

PACS number(s): 61.30.Cz, 61.30.Gd

In the last several decades the surface anchoring effect in nematic liquid crystals (NLC) was extensively studied [1,2]. Many techniques have been invented to build appropriate anchoring properties, and many methodologies have been established to measure the energies relevant to interfacial anchorage. Unfortunately, the theoretical recognition may not be satisfactory. In the early stage, strong anchoring was used to depict the NLC-substrate interfaces, which assumes that the director at the surface is fixed at the easy direction. However, in most cases the surface coupling is not so strong, and hence the concept of weak anchoring has been introduced. Rapini and Papoular (RP) built a simple phenomenological expression for the interfacial energy of homeotropic anchoring per unit area [3]:  $g_s = A \sin^2 \Phi_0$ , where  $\Phi_0$  is the polar angle of the director at the surface, and the constant  $A$  is termed anchoring strength or anchoring energy. After that, many attempts had been made to generalize the RP energy in order to describe the planar and tilt anchoring [4–7]. Until now the situation has been quite perplexing. Becker *et al.* considered a surface with weak polar and strong azimuthal anchoring [5]. Sugimura *et al.* used an interfacial energy with a single coupling constant [6], but their argument is criticized due to the incapability of distinguishing between azimuthal and polar coupling. Beica *et al.* [7] significantly improved the RP model, however, their contribution is still incomplete as a second-order spherical-harmonic model (see below); furthermore, their approach fails in applying to the homeotropic surface with in-plane anisotropy [8], as with the substrate used in Refs. [9] and [10].

In this Rapid Communication, employing a spherical-harmonic expansion, we build a second-order formula of the anisotropic interfacial energy. It is clear that the energies used in [3–7] are all special cases of this generalized formula. To study its consequences, we apply it to a twisted nematic slab sandwiched between two unidirectional planar anchoring surfaces [11,12], and to the voltage-controlled-twist (VCT) effect [9]. For the former, we show that our study can approach the common case in which the azimuthal and polar anchoring energies are both finite and distinct from each other. For the latter, the generalized surface energy properly yields the voltage-dependent twist and saturation behaviors.

As a function of directions,  $g_s$  has been developed into a series of spherical harmonics with respect to the surface nor-

mal [2]. To make it clear, we emphasize here that the equivalence of  $\vec{n}$  and  $-\vec{n}$  leads to centrosymmetry of  $g_s$ :  $g_s(\vec{n}) = g_s(-\vec{n})$ . This means that  $g_s$  is a function defined on the whole solid angle, although the liquid crystal exists only on one side of the interface. A consequence of the centrosymmetry is that any odd-order term disappears spontaneously in a series expansion of  $g_s$ .

With a single easy direction  $\vec{\epsilon}(\theta_0, \phi_0)$  (Fig. 1),  $g_s$  becomes such a function: it is centrosymmetric, and it has two minima in  $\vec{\epsilon}$  and  $-\vec{\epsilon}$ . Now we expand  $g_s$  into a series of spherical harmonics with respect to the *easy axis*  $\vec{\epsilon}$ . The second-order result is [13]

$$g_s(\Theta, \Phi) = \sum_{l=0}^2 \sum_{m=-l}^l g_{lm} Y_{lm}(\Theta, \Phi), \quad g_{l-m} = g_{lm}^*. \quad (1)$$

Here  $\Theta$  and  $\Phi$  are the polar and azimuthal angles with respect to  $\vec{\epsilon}$ . In Eq. (1),  $g_{00}$  is the isotropic part and can be neglected. The  $l=1$  terms disappear due to the breaking of centrosymmetry. Since  $Y_{20}(\Theta, \Phi) = (3 \cos^2 \Theta - 1)/2$ , we know that the  $g_{20}$  term just corresponds to the single-constant energy [6]

$$\cos^2 \Theta = (\vec{n} \cdot \vec{\epsilon})^2. \quad (2)$$

We have  $g_{21}=0$ , since a nonzero  $g_{21}$  would break the definition that the easy direction  $\vec{\epsilon}(\Theta=0)$  is the energy minimum [14]. This is a significant simplification. If  $g_{22}=g_{22,R} + i g_{22,I}$ , the  $g_{22}$  terms become

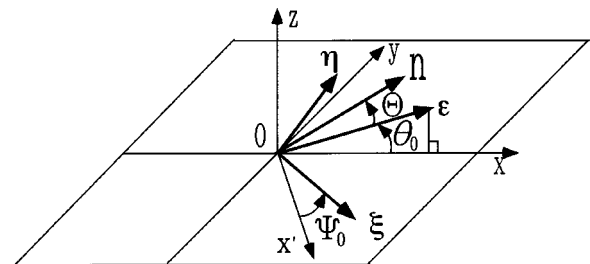


FIG. 1. Schematic of anisotropic surface anchoring. Here  $\phi_0 = 0$ , and  $\Phi$  (not marked) is the angle between planes  $\epsilon O x'$  and  $\epsilon O n$ .

$$g_{22}Y_{22}(\Theta, \Phi) + \text{c.c.} = 4|g_{22}|\sin^2 \Theta \cos^2(\Phi - \Psi_0) - 2|g_{22}|\sin^2 \Theta, \quad (3)$$

where  $\Psi_0 = -\arctan(g_{22,I}/g_{22,R})/2$ . In Eq. (3) some constant factors are neglected in the definition of spherical harmonics. Merging the second term on the right-hand side of Eq. (3) with Eq. (2), we get the second-order form of the anchoring energy

$$g_s(\Theta, \Phi) = W_\xi \sin^2 \Theta \cos^2(\Phi - \Psi_0) + W_\eta \sin^2 \Theta \sin^2(\Phi - \Psi_0) = W_\xi(\vec{n} \cdot \vec{\xi})^2 + W_\eta(\vec{n} \cdot \vec{\eta})^2, \quad (4)$$

where some constants are discarded.  $(\vec{\xi}, \vec{\eta}, \vec{\epsilon})$  is an orthonormal vector triplet (Fig. 1), with Euler angles  $(\phi_0, \pi/2 - \theta_0, \Psi_0)$  rotating from the elementary triplet  $(\hat{x}, \hat{y}, \hat{z})$ . Here  $W_\xi$  and  $W_\eta$  are both positive, since  $\vec{\epsilon}$  is the easy axis. Equation (4) implies the presence of surface-induced nematic biaxiality, in that the deviation of director  $\vec{n}$  away from the easy axis  $\vec{\epsilon}$  in the  $(\vec{\epsilon}, \vec{\xi})$  plane costs  $W_\xi$ , whereas in  $(\vec{\epsilon}, \vec{\eta})$  plane the cost is  $W_\eta$ . It is instructive to point out the improvement of our approach upon the contribution of Beica *et al.* [7]: Beica *et al.* took it for granted that  $\Psi_0 = 0$ , yet our analysis demonstrates that for the general case, the anchoring triplet may be in a more complicated angular position with respect to the elementary triplet  $(\hat{x}, \hat{y}, \hat{z})$ .

Equation (4) builds a simple description of the anisotropic interfacial energy. Now consider the unidirectional planar anchoring case. Assuming  $\vec{\epsilon} = \hat{x}$ , we know that  $\vec{\xi}$  and  $\vec{\eta}$  are two unit vectors in the  $y$ - $z$  plane. If we postulate further the  $y \leftrightarrow -y$  symmetry of the anchoring surface, which leads to  $\Psi_0 = 0$ , Eq. (4) can be simplified to

$$g_s = W_a(\vec{n} \cdot \hat{y})^2 + W_p(\vec{n} \cdot \hat{z})^2. \quad (5)$$

$W_a$  and  $W_p$  refer to the azimuthal and polar anchoring strengths, respectively. Nevertheless, if the surface is asymmetric about the  $y \leftrightarrow -y$  reflection due to oblique SiO evaporation [15] or asymmetric periodic surface grating [16], a nonzero  $\Psi_0$  may exist in coarse-grained treatment (for instance, in Ref. [16], for the homogeneous alignment cases,  $\Psi_0$  just corresponds to the pretilt).

Another case worth mentioning is the homeotropic surface with in-plane anisotropy, used in the VCT effect [9] and homeotropic to twisted planar transition [10]. Applying Eq. (4) to this case we get

$$g_s = W_x(\vec{n} \cdot \hat{x})^2 + W_y(\vec{n} \cdot \hat{y})^2. \quad (6)$$

Here  $W_x$  and  $W_y$  are the zenithal anchoring strengths corresponding to the deformations in the  $x$ - $z$  and  $y$ - $z$  planes, respectively. Their difference,  $W_x - W_y$ , is the azimuthal energy breaking, and for the grooved surface it just corresponds to the Berreman effective anchorage [17]. To build an intuitive impression, in Fig. 2 we show the energy-direction graph of a planar-anchoring surface defined by Eq. (5). In the

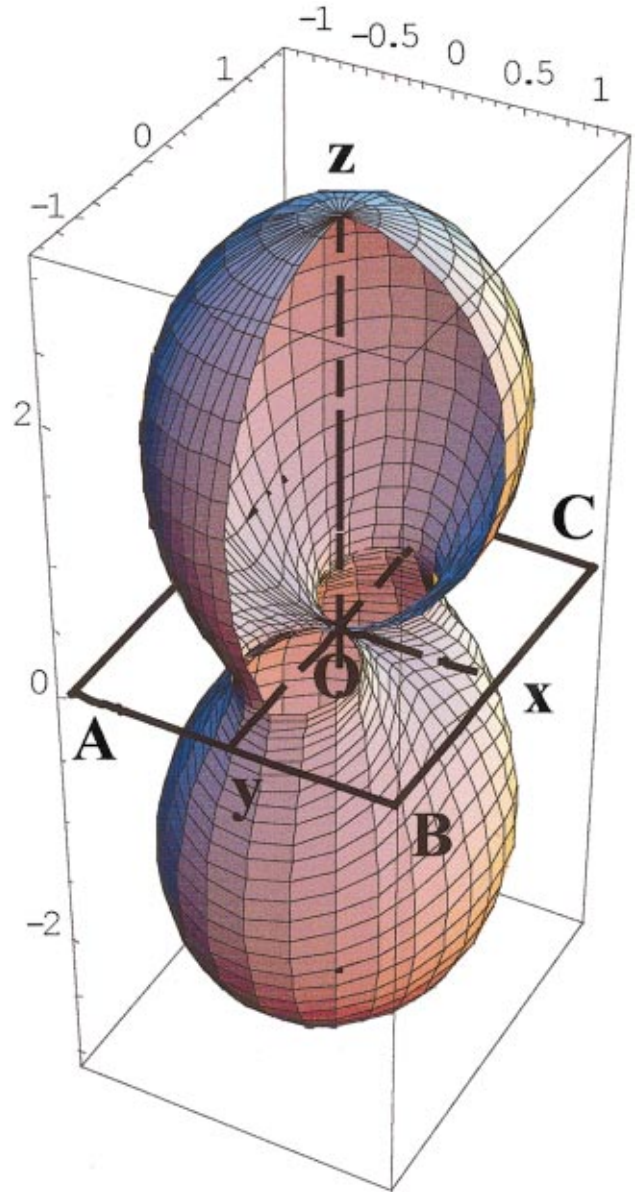


FIG. 2. (Color) A cut-away view of the energy-direction graph for a planar anchoring surface  $ABC$  depicted by Eq. (5), with  $W_a = 1$  and  $W_p = 3$  (in arbitrary units). The length of the radius vector from  $O$  to any point at the curved surface represents the interfacial energy  $g_s$  in that direction.

general case it may be more complicated geometrically, since only second-order terms are included here.

Now we apply this interfacial energy to some specific cases to demonstrate its consequences. First, we consider a chiral NLC slab located between two identical planes  $z = 0$  and  $z = l$ , yielding unidirectional planar anchorage with their easy axes in the directions of  $\phi = 0$  and  $\phi = \phi_t$ , respectively. The free energy of the slab is expressed as [18]

$$F = \int g_b dv + \int g_s^- ds^- + \int g_s^+ ds^+, \quad (7)$$

where  $g_s^\pm$  are the adaptations of Eq. (5) to the substrate surfaces, and  $g_b$  is the bulk energy density

$$g_b = \frac{1}{2} [k_{11}(\nabla \cdot \vec{n})^2 + k_{22}(\vec{n} \cdot \nabla \times \vec{n} + 2\pi/p_0)^2 + k_{33}[\vec{n} \times (\nabla \times \vec{n})]^2] - \frac{\Delta\chi}{2} (\vec{n} \cdot \vec{H})^2. \quad (8)$$

Here  $k_{11}$ ,  $k_{22}$ , and  $k_{33}$  are elastic constants,  $p_0$  and  $\Delta\chi$  are respectively the pitch and the anisotropic part of the diamagnetic susceptibility of the chiral NLC and  $H$  is the magnetic field in the  $\hat{z}$  direction.

Our aim is to attain the Fréedericksz threshold field  $H_F$  and the saturation field  $H_S$ . We performed a variational calculation to build the equilibrium equations, and solved them under certain limiting conditions. Here we just briefly show the results. We define  $\lambda = \pi k_{11}/(2lW_p)$ ,  $\gamma = W_a/W_p$ ,  $u' = H_F/H_c$ , and  $u'' = H_S/H_c$ , where  $H_c = \pi(k_{11}/\Delta\chi)^{1/2}/l$  is the threshold field for an untwisted nematic slab ( $\phi_t=0$ ) with rigid boundary coupling. The reduced threshold field is given by

$$u' = \left[ X^2 - \frac{(2k_{22} - k_{33})\Delta\phi^2}{\pi^2 k_{11}} + \frac{4lk_{22}\Delta\phi}{\pi p_0 k_{11}} \right]^{1/2}, \quad (9)$$

where  $\Delta\phi = \phi_t - 2\phi^0$ ,  $\phi_0$  and  $X$  are solutions to Eqs. (10) and (11),

$$\phi_t - 2\phi^0 - \frac{2\pi l}{p_0} = \frac{\pi\gamma k_{11}}{2\lambda k_{22}} \sin 2\phi^0, \quad (10)$$

$$(1 - \gamma \sin^2 \phi^0)/\lambda = X \tan(\pi X/2). \quad (11)$$

And the reduced saturation field is given by

$$u'' = \left\{ \frac{k_{33}}{k_{11}} \left[ Y^2 + \left( \frac{2lk_{22}}{p_0 k_{33}} \right)^2 \right] \right\}^{1/2}, \quad (12)$$

in which  $Y$  is defined by

$$\frac{1}{\gamma} \cosh^2 \left( \frac{\pi}{2} Y \right) \left[ 1 - \frac{k_{33}}{k_{11}} \lambda Y \tanh \left( \frac{\pi}{2} Y \right) \right] \times \left[ 1 - \frac{k_{11}}{k_{33}} \frac{1 - \gamma}{\lambda Y} \tanh \left( \frac{\pi}{2} Y \right) \right] = \sin^2 \left( \frac{\phi_t}{2} - \frac{\pi l k_{22}}{p_0 k_{33}} \right). \quad (13)$$

In Fig. 3(a), the  $\lambda$  and  $\gamma$  dependences of the threshold and saturation fields are shown for a  $90^\circ$  twisted NLC layer, with the same material parameters as those used in Refs. [5] and [6]. Besides the curves of  $\gamma \rightarrow \infty$  and  $\gamma = 1$ , which repeat the previous results by Becker *et al.* [5] and Sugimura *et al.* [6], we additionally plot the curves for  $\gamma = \frac{1}{10}$ , which simulate the realistic case that the azimuthal anchoring is one or two orders weaker than the polar coupling, and  $\gamma = 0$  as a limit case, corresponding to the degenerate planar anchorage.

Second, we study the VCT effect. In Ref. [9], the authors analyzed the VCT effect using the finite-element method. Berreman's seminal work [17] indicated that the profile effect may be equivalent to an anisotropic surface energy. Along this route, we use Eq. (6) to simulate the anchoring effect of the grating surface. The opposite substrate builds a rigid planar boundary condition ( $\theta^+ = 0$ ,  $\phi^+ = 0$ ). The mag-

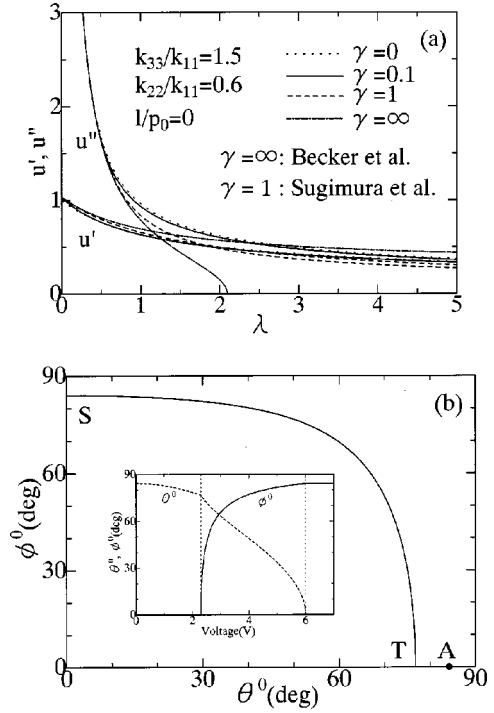


FIG. 3. (a)  $\lambda$  and  $\gamma$  dependences of the reduced threshold ( $u'$ ) and saturation ( $u''$ ) fields of a  $90^\circ$  twisted NLC slab. (b) The VCT effect. As the voltage increases from 0 to  $V_T$  to  $V_S$ , the system goes from A to T to S. The inset shows the voltage dependence of  $\theta^0$  and  $\phi^0$ . The parameters used are  $k_{11} = 16.7$  pN,  $k_{22} = 8.0$  pN,  $k_{33} = 18.1$  pN,  $p_0 = \infty$ ,  $\Delta\epsilon = -4.2$ ,  $W_x = 27.9 \times 10^{-6}$  J/m<sup>2</sup>,  $W_y = 15.8 \times 10^{-6}$  J/m<sup>2</sup>, and  $l = 4.7$   $\mu$ m.

netic action in Eq. (8) is replaced by the electric energy  $\frac{1}{2} |\Delta\epsilon| \epsilon_0 (\vec{n} \cdot \vec{E})^2$ . Here  $\Delta\epsilon$  and  $\epsilon_0$  are the dielectric anisotropy and the permittivity of free space. For simplicity, we made an approximation to replace the local field  $E$  with an average field  $\bar{E} = V/l$ , with  $V$  being the voltage (this approximation is proper if  $|\Delta\epsilon| \ll \epsilon_\perp$ , and is sufficient at present to predict the VCT effect, since the key point is the interfacial energy of the grating surface).

A series of derivations yield the following equations which define the voltage dependence of the director  $\vec{n}^0(\theta^0, \phi^0)$  at the grating surface,

$$C_1 = -(W_x - W_y) \cos^2 \theta^0 \sin 2\phi^0, \quad (14)$$

$$C_2 = (W_x \cos^2 \phi^0 + W_y \sin^2 \phi^0)^2 \sin^2 2\theta^0 / f + C_1^2 / h(\theta^0) - |\Delta\epsilon| \epsilon_0 \bar{E}^2 \sin^2 \theta^0, \quad (15)$$

$$l = \int_0^{\theta^0} [f(\theta)/N(\theta)]^{1/2} d\theta, \quad (16)$$

$$\phi^0 = - \int_0^{\theta^0} C_1 [f(\theta)/N(\theta)]^{1/2} / h(\theta) d\theta. \quad (17)$$

Here  $f(\theta) = k_{11} \cos^2 \theta + k_{33} \sin^2 \theta$ ,  $h(\theta) = \cos^2 \theta (k_{22} \cos^2 \theta + k_{33} \sin^2 \theta)$ , and

$$N(\theta) = C_2 + |\Delta\epsilon| \epsilon_0 \bar{E}^2 \sin^2 \theta - C_1^2 / h(\theta). \quad (18)$$

Noting that the director begins to twist at  $V_T=2.3$  V, and saturates at  $V_S=6.0$  V in Fig. 3(a) in [9], and using the parameters enumerated there, we can evaluate that  $W_x=27.9 \times 10^{-6}$  J/m<sup>2</sup> and  $W_y=15.8 \times 10^{-6}$  J/m<sup>2</sup>, which are reasonable values for homeotropic alignment. The in-plane anisotropy  $W_x-W_y$  seems small compared with the Berreman evaluation, yet this is not a serious problem since Faetti [19] offered a reasonable explanation. Then by computation the  $\theta^0-V$ ,  $\phi^0-V$  curves and the  $\phi^0-\theta^0$  diagram are drawn in Fig. 3(b). As the voltage increases from 0 to  $V_T$  to  $V_S$ , the

system goes from  $A$  to  $T$  to  $S$  in the  $\phi^0-\theta^0$  diagram, exhibiting a typical continuous transition. A meaningful implication of this equivalent treatment is that the homeotropic substrate used in a VCT cell may be prepared by other methods than grating [10], since the essential point is the in-plane anisotropy.

In summary, we have built a two-constant formula as a generalization of the RP model. Some significant cases have been discussed. Our analysis on the twisted NLC device and the VCT effect shows that this energy is useful in depicting anisotropic interfacial phenomena.

- 
- [1] A. A. Sonin, *The Surface Physics of Liquid Crystals* (Gordon and Breach, London, 1995).
- [2] B. Jérôme, *Rep. Prog. Phys.* **54**, 391 (1991).
- [3] A. Rapini and M. Papoular, *J. Phys. (Paris) Colloq.* **30**, C4-54 (1969).
- [4] J. Nehring, A. R. Kmetz, and T. J. Scheffer, *J. Appl. Phys.* **47**, 850 (1976).
- [5] M. E. Becker, J. Nehring, and T. J. Scheffer, *J. Appl. Phys.* **57**, 4539 (1985).
- [6] A. Sugimura and Z. Ou-Yang, *Phys. Rev. E* **51**, 784 (1995); A. Sugimura, G. R. Luckhurst, and Z. Ou-Yang, *ibid.* **52**, 681 (1995).
- [7] T. Beica, S. Frunza, R. Moldovan, and D. N. Stoenescu, *Mol. Cryst. Liq. Cryst.* **301**, 39 (1997).
- [8] In homeotropic case, the easy direction  $\vec{n}_S$  is parallel to the normal to the surface  $\mathbf{k}$ . Hence,  $\vec{n}_{ST}$  and  $\vec{n}_{SH}$ , the other two vectors defined by Beica *et al.*, disappear.
- [9] G. P. Bryan-Brown, C. V. Brown, I. C. Sage, and V. C. Hui, *Nature (London)* **392**, 365 (1998).
- [10] S.-W. Suh, S. T. Shin, and S.-D. Lee, *Mol. Cryst. Liq. Cryst.* **302**, 163 (1997).
- [11] F. M. Leslie, *Mol. Cryst. Liq. Cryst.* **12**, 57 (1970).
- [12] M. Schadt and W. Helfrich, *Appl. Phys. Lett.* **18**, 127 (1971).
- [13] C. G. Gray and K. E. Gubbins, *Theory of Molecular Fluids* (Clarendon, Oxford, 1984).
- [14] Noting that  $\partial[g_{21}Y_{21}(\Theta, \Phi) + \text{c.c.}]/\partial\Theta|_{\Theta=0} = g_{21}e^{i\phi} + \text{c.c.} \neq 0$ , we know that  $\Theta=0$  is not a minimal-energy direction, if  $g_{21} \neq 0$ .
- [15] J. L. Janning, *Appl. Phys. Lett.* **21**, 173 (1972).
- [16] C. V. Brown, M. J. Towler, V. C. Hui, and G. P. Bryan-Brown, *Liq. Cryst.* **27**, 233 (2000).
- [17] D. W. Berreman, *Phys. Rev. Lett.* **28**, 1683 (1972).
- [18] P. G. de Gennes and J. Prost, *The Physics of Liquid Crystals*, 2nd ed. (Clarendon, Oxford, 1993).
- [19] S. Faetti, *Phys. Rev. A* **36**, 408 (1987).